TITLE: **CHANGES IN U(VI) SPECIATION UPON SORPTION ONTO MONTMORILLONITE FROM AQUEOUS AND ORGANIC SOLUTIONS**

AUTHOR(S): CATHERINE CHISHOLM-BRAUSE, DAVID E. MORRIS, P. GARY ELLER, TOM BUSCHER, AND STEVEN D. CONRADSON

SUBMITTED TO: 15TH INTERNATIONAL SYMPOSIUM ON THE SCIENTIFIC BASIS FOR NUCLEAR WASTE MANAGEMENT

Los Alamos

Los Alamos National Laboratory
Los Alamos, New Mexico 87545

MASTER

CHANGES IN U(VI) SPECIATION UPON SORPTION ONTO MONTMORILLONITE FROM AQUEOUS AND ORGANIC SOLUTIONS

Catherine Chisholm-Brause, David E. Morris, P. Gary Eller, Tom Buscher, and Steven D. Conradson

Los Alamos National Laboratory
Los Alamos, New Mexico   87545 USA

ABSTRACT

The speciation of UO_2^{2+} and UO_2^{2+}/TBP mixtures has been investigated in solution and intercalated with the reference smectite clay SAz-1 using x-ray absorption, Raman, and luminescence spectroscopies. Neither aquated UO_2^{2+} nor its TBP complex undergoes any detectable changes in uranium oxidation state on intercalation. Further, at the pH values employed in this work, there is no evidence for hydrolysis of the uranium species to generate dimeric or higher order uranium oligomers. However, we do find indications that the structures of the solution complexes are altered on intercalation, particularly for the UO_2^{2+}/TBP system. In addition, several lines of evidence suggest that, at the loading levels used in this study, the uranyl species may be interacting with two or more spectroscopically distinguishable sites on SAz-1.

1

Introduction

Past waste management practices at U.S. Department of Energy complexes have resulted in significant levels of organic solvents, neutral donor extractants, and actinides in the underlying soil and groundwater. To evaluate the mobility and fate of such "co-contaminant" (actinide/organic) wastes in clay-rich soils and groundwaters, we have conducted spectroscopic experiments on a model system: U(VI) in aqueous or 20% tributyl-phosphate (TBP)/docecane solutions, and sorbed on montmorillonite (SAz-1 from the Missouri Clay Repository) from these solutions.

Tributylphosphate (TBP) is a complexing organic reagent common to the contaminant inventories at a number of U.S. Department of Energy sites. TBP is key high-volume reagent in the nuclear complex, being used widely with hydrocarbon diluents as the extractant in reprocessing of spent fuel (the PUREX process)[2] and in combination with a chelating phosphonate for lanthanide/actinide group separations (the TRUEX process) [2,3]. Subsurface contamination by TBP and related neutral-donor extractants has been identified at U.S. Department of Energy transuranic processing sites such as the Hanford and Savannah River facilities, and at low-level waste disposal sites including Maxey Flats, Kentucky and West Valley, New York [4-6]. More specifically, large TBP/solvent releases to the environment have occurred at the Hanford site, yet TBP has not been detected in near-surface groundwaters [7]. This interesting observation could be related to TBP uptake by soil and/or rock column constituents.

The influence of neutral-donor extractants on the sorption properties and the subsurface migration behavior of radionuclides is largely unknown, even with dominant soil constituents such as clays. We are characterizing the speciation properties of actinides and transition metals in the presence of neutral donor extractants at the interface between solutions and common subsurface mineral matrices. We have chosen the smectite clay SAz-1 as our initial reference substrate because it is representative of the ubiquitous 2:1 layered clay materials found at many contaminant sites in the U.S. Recently we found that TBP is taken up extensively by SAz-1 with large concomitant swelling of the clay interlayer region [8]. It appears that a major fraction of the intercalated TBP undergoes a bonding interaction with interlayer cations.

2

Uranium is an important actinide contaminant commonly found in environmental releases, particularly plumes associated with mill tailings operations [9]. Frequently pore fluid pH values less than 2-3 are encountered, and under oxidizing conditions dissolved uranium is predominantly in the U(VI) (uranyl) form and is quite mobile [10]. In this oxidation state, uranium has an important advantage for speciation studies. Namely, the O=U=O moiety is a highly characteristic chromophore in vibrational, absorption, and luminescence spectroscopies. In fact, it is one of the few species that possesses vibronically resolved electronic spectra in fluid solutions at room temperature. The ground-state U=O vibrational energy (derived either from the Raman spectrum or the luminescence spectrum) and other spectroscopic parameters (e.g., electronic origin energies, linewidths, and excited-state lifetimes) are known to vary greatly depending on the coordination environment of UO_2^{2+} [11-17]. Thus, these spectroscopic probes provide valuable speciation information that can be used to complement more explicit structural data derived from x-ray absorption spectroscopy.

The importance of providing more detailed, molecular-level descriptions of surface and interfacial contaminant speciation has been stressed in recent reports [18,19]. Toward this end, in this report we present x-ray absorption, Raman, and luminescence spectroscopic results for UO_2^{2+} and UO_2^{2+}/tributylphosphate mixtures in solution and sorbed onto the reference smectite SAz-1.

Experimental

Sample Preparations

The reference smectite clay SAz-1 from Cheto, Arizona, was obtained from the University of Missouri Source Clay Repository. This is a relatively pure, readily expandable, high cation exchange capacity clay with Ca^{2+} as the dominant interlayer cation [20]. Most experiments were conducted with the clay in the form in which it was received. In some experiments the clay was size fractionated by sedimentation according to published procedures [21] prior to use, and the small fraction (0.2 to 5 uM) was used for sample preparations. We observed no significant differences in results between experiments using the as-received and size-fractionated materials. Uranyl solutions were prepared from solid $UO_2(NO_3)_2 \cdot 6H_2O$ in all cases. Both the TBP and the dodecane diluent

were purified by distillation prior to use. The absence of impurities in these reagents was confirmed by NMR and FTIR methods. TBP solutions in dodecane were 20% by volume. The clay intercalation reactions were carried out by gently mixing the clay (typically 1 g sample) with ~ 10 mL of the appropriate intercalation reagent for periods from 24 to 120 hrs at room temperature. Intercalation was visually noticed to occur within a few minutes of contact. No effort was made to exclude CO_2 from the solutions since carbonate uptake is not expected to be important at the low pH values used. The resulting clay suspensions were centrifuged and washed a minimum of three times with either deionized water (for aqueous treatments) or pentane or hexane (for 20% TBP/dodecane treatments) to remove unbound, excess reagents. Some samples were allowed to air-dry (ambient temperature and humidity were ~ 22 °C and ~10 % respectively) prior to investigation.

Spectroscopic Measurements

Raman and luminescence spectra were obtained on a SPEX Industries Model 1403 scanning double monochromator equipped with 1800 gr/mm holographic gratings, an RCA C31034 photomultiplier tube, and Stanford Research Model SR400 photon counting electronics. A Spectra Physics Model 2045 continuous wave argon Ion laser was used for excitation of both Raman and luminescence spectra. Raman spectra were obtained using the exciting line at either 3638 Å, 4579 Å, or 4880 Å. All luminescence spectra were obtained using 3638 Å excitation. Both Raman scattered and emitted light were collected using 180° backscattering geometry. Both wet and dry clay samples and solutions were contained in 5 mm bore NMR tubes.

Uranium L_{III}-edge x-ray absorption spectra were collected at the National Synchrotron Light Source at Brookhaven National Laboratory on beam line X8C. Si(220) double-crystals were used for monochromatization. Higher energy harmonic reflections were rejected by detuning the primary beam by 50%. Typical beam currents were 100 to 180 mA. The spectra of reference solids and solutions, and sorption samles were collected in transmission mode. The signal-to-noise ratio was increased by averaging 2 to 14 spectra. Analysis of raw x-ray absorption data to radial structure functions was carried out by previously described procedures [23,24].

Results and Discussion

The radial structure functions derived from the uranium EXAFS data for several of the UO_2^{2+} species are shown in Figure 1. The structural parameters obtained from the curve fits of the EXAFS data are summarized in Table I. Note the excellent agreement between the EXAFS data for solid uranyl nitrate and the neutron diffraction result [26]. The following conclusions can be drawn from the x-ray absorption data:

(1) The spectra of all samples (with the possible exception of the UO_2^{2+}/TBP/SAz-1 sample, *vide infra*) exhibit the same first-shell structure demonstrating that (a) no redox processes have occurred to change the uranium valence, and (b) the O=U=O structural moiety has remained intact under a variety of conditions. This conclusion is further supported by the near-edge x-ray absorption spectra (XANES) which were identical for all samples.

(2) For all samples in solution, the coordination numbers and average bond distances for the equatorial ligands are consistent with expectation. In particular, the stoichiometry of the TBP complex of uranyl nitrate in organic solutions (e.g., dodecane) is expected to be $UO_2(NO_3)_2 \cdot 2TBP$ [2]. Thus, the equatorial coordination number of six (2 oxygens from each nitrate and 1 oxygen from each TBP) compares favorably with the EXAFS value of 5.8. Under the aqueous conditions employed in this work (i.e., acidic solutions with nitrate concentrations less than or equal to ~1 M), the nitrate ions should not be retained within the inner coordination sphere of the uranyl, and the equatorial coordination number of about 9 likely represents the coordination of water molecules.

(3) It is known that UO_2^{2+} readily dimerizes in aqueous solution beginning at about pH 2.5 [27]. However, no discernible second-shell features attributable to U-U interactions were seen in any of UO_2^{2+}/SAz-1 the EXAFS data. Thus, polymerization or other precipitation and/or clustering processes appear to be absent under the conditions employed in the present study.

For the clay samples treated with uranyl ion, with and without TBP, the EXAFS data suggest that the speciation is more complicated than in the reference solids and the solutions. For the clay sample prepared from aqueous UO_2^{2+} solution, the axial structure parameters remain consistent with an O=U=O moiety. However, the

equatorial coordination number is anomalously low. For the clay sample prepared with aqueous UO_2^{2+} and 20 % TBP/dodecane present, even the axial coordination number is anomalous. The broadened and flattened amplitudes found in the radial structure functions (e.g., Fig. 1D) suggest some type of static or thermal disorder in these systems.

A portion of the Raman spectrum of the UO_2^{2+}/TBP complex (presumed to be $UO_2(NO_3)_2 \cdot 2TBP$, vide supra) in 20% TBP/dodecane solution is compared to that of aquated UO_2^{2+} (from the nitrate salt) in aqueous solution in Figure 2 A and B. Note that the totally symmetric U=O vibration has shifted to lower energy by ~12 cm^{-1} upon TBP complexation of uranyl. Similarly, the nitrate vibrational mode has shifted to lower energy by ~ 29 cm^{-1} on going from the uncomplexed form in aqueous solution to the complexed form in the organic medium. The decrease in the U=O frequency upon TBP complexation is likely indicative of a slight increase in the U=O bond length in the complex. A number of the Raman vibrational modes of TBP are also perturbed upon complexation to UO_2^{2+}, but there is not sufficient published data on the influence of metal-ion complexation on Raman vibrational energies of TBP to draw meaningful conclusions from the present data.

The Raman spectrum of SAz-1 treated with aqueous UO_2^{2-} solution is shown in Figure 2 C. Note that there is an apparent splitting of the U=O vibrational band into two new bands, neither of which corresponds exactly in energy to the aqueous U=O band. Note also that the characteristic, intense vibrational band for NO_3^- is absent in the clay spectrum, indicating that nitrate is probably not incorporated into the clay under these conditions. (The origin of the band at ~ 708 cm^{-1} in the clay spectrum is unknown.) The splitting of the U=O vibrational band could be the result of several effects. However, the magnitude of the splitting (~ 26 cm^{-1}) allows us to assess the likelihood of two of the more probable effects; namely redox reactions to generate UO_2^+ species and/or hydrolysis reactions to generate dimeric or trimeric species. Upon reduction of UO_2^{2+} to UO_2^+, the vibrational frequency of the U=O mode typically decreases by ~ 50 cm^{-1} [14]. The vibrational frequency change for this mode between UO_2^{2+} and the dimer $(UO_2)_2(OH)_2^{2+}$ is only ~18 cm^{-1} [13, 28]. Thus neither reduction nor dimerization seems plausible to account for the observed band splitting in the UO_2^{2+} SAz-1 spectrum. Note that the absence of redox and/or hydrolysis mechanisms is consistent with the interpretation of the x-ray absorption data. An alternative explanation

for the observed band splitting is the existence of spectroscopically distinguishable multiple sorption sites for UO_2^{2+} on the clay. Attempts were made to obtain the Raman spectrum of the UO_2^{2+}/TBP complex intercalated into SAz-1. Unfortunately, this intercalation complex luminesces too intensely even in the ultraviolet (364 nm) to allow discrimination of Raman scattered light.

The luminescence spectra for UO_2^{2+} species in several environments are shown in Figures 4. Surprisingly, the emission from the UO_2^{2+}/TBP complex in organic solution (Fig. 4 C) is unstructured and very effectively quenched in comparison to the other UO_2^{2+} species. For example, UO_2^{2+}/TBP mixtures intercalated into SAz-1 give rise to an intense uranyl emission (Fig. 4 D). This strongly suggests that there are important structural differences between the UO_2^{2+}/TBP complex in solution (i.e., $UO_2(NO_3)_2 \cdot 2TBP$) and the species sorbed on the clay. The spectra in Figure 4 A-C are all characterized by prominent vibronic structure in the emission band. It has been reported that UO_2^{2+} in perchlorate media has luminescence from two excited states [15-17]. However, the present results can be interpreted on the basis of only a single emitting excited state. The spectrum of aqueous UO_2^{2+} (Fig. 4 A) clearly shows two progressions, but these appear to arise from two vibrational modes rather than a single vibrational mode in two excited electronic states. In fact, spectral fitting using time-dependent theories of spectroscopy [29] has been used to reproduce this spectrum assuming a single emitting state and two vibrational modes.

A summary of the important luminescence and Raman spectral data is given in Table II. Note that there is excellent agreement between the vibrational frequency for the aqueous UO_2^{2+} species determined by Raman spectroscopy (873 cm^{-1}) and that derived from the vibronic spacing (870 cm^{-1}) in the luminescence spectrum. The agreement between Raman and luminescence data is not as good for the aqueous UO_2^{2+} species intercalated into SAz-1. Here only a single vibronic frequency is resolved in the luminescence spectrum compared to two distinct Raman frequencies. Note however that the vibronic frequency (840 cm^{-1}) is close to the observed Raman values (855 and 881 cm^{-1}). No such comparison can be made for the UO_2^{2+}/TBP species intercalated into SAz-1 because of the inability to collect a Raman spectrum (vide supra). It is noteworthy that the vibronic spacing for the clay species (750 cm^{-1}) is dramatically lower than the Raman value measured for the UO_2^{2+}/TBP complex in

7

solution (861 cm^{-1}), again suggesting a significant difference between the structures of the solution complex and those found in the clay environment. Note also (Fig. 4) that the vibronic linewidths for the clay species are greater than that of the aqueous species. Once again, this may be a manifestation of multiple sorption sites for UO_2^{2+} species on the clay. The increased line width (compared to the aqueous solution spectrum) would be the result of the superposition of slightly different luminescence spectra from the species in each site. This possibility is presently under investigation using spectral fitting to deconvolute the observed spectra.

CONCLUSIONS

The spectroscopic data presented herein demonstrate that UO_2^{2+} and its TBP complexes can be intercalated into the smectite clay SAz-1 without apparent changes in uranium oxidation state, and, at the low pH values employed in this work, apparently without hydrolysis of the uranium species to form oligomers. There are however indications that the structures of the solution complexes become altered on intercalation, particularly for the UO_2^{2+}/TBP complex(es). Finally, several lines of evidence suggest that, at the loading levels used in this study, the uranyl species may be interacting with two or more spectroscopically distinguishable sites on SAz-1.

ACKNOWLEDGEMENTS

REFERENCES

1. McCarthy, J.F.; Zachara, J.M. *Env. Sci. Tech.* **1989**, 3, 496.
2. Schulz, W.W.; Navratil, J.D.; Talbot, A.E. (eds.) <u>Science and Technology of Tributyl Phospate</u>, Volumes 1-3, CRC Press, Columbus, (1984).
3. Katz, J.J.; Seaborg, G.T.; Morss, L.R. (eds.) <u>Chemistry of the Actinide Elements</u>, Volumes 1 and 2, Chapman and Hall, New York (1986).
4. Killian, T.H. Kolb, N.L.; Corbo, P.; Marine, I.W. "Environmental Information Document. H-Area Seepage Basin," Savannah River Laboratory Report DPST-85-706.
5. Francis, A.J.; Iden, C.R.; Nine, B.J.; Chang, C.K. *Nucl. Tech*, **1980**, 50, 158.
6. Valenti, P.J.; McVay, C.W.; Bourgeois, P. *Trans. Amer. Nucl. Soc.*, **1986**, 52, 55.
7. Stenner, R.D.; Cramer, K.H.; Higley, K.A.; Jette, S.J.; Lamar, D.A.; McLaughlin, T.J.; Sherwood, D.R.; Van Houten, N.C. Pacific Northwest Laboratory report PNL-6456, Vol. 3 (1988).
8. Eller, P.G.; Morris, D.E.; Buscher, C.T.; Bish, D.E.; King, C.B. submitted to *Environ. Sci. Tech.*
9. Merritt, R.C. "The Extractive Metallurgy of Uranium," <u>Colorado School of Mines Research Institute</u>, Golden, CO (1971).
10. Weig el, F. in <u>Chemistry of the Actinide Elements</u>, Katz, J.J.; Seaborg, G.T.; Morss, L.R. (eds.) Chapman and Hall, New York (1986), Chapter 5.
11. Ohwada, K. *J. Coord. Chem.* **1978**, 8, 35.
12. Brooker, M.H.; Huang, C.-H.; Sylwestrowicz, J. *J. Inorg. Nucl. Chem.* **1980**, 42, 1431.
13. Toth, L.M.; Begun, G.M. *J. Phys. Chem.* **1981**, 85, 547.
14. Madic, C.; Hobart, D.E.; Begun, G.M. *Inorg. Chem.* **1983**, 22, 1494.
15. Bell, J.T.; Biggers, R.E. *J. Molec. Spec.* **1965**, 18, 247.
16. Bell, J.T.; Biggers, R.E. *J. Molec. Spec.* **1967**, 22, 262.
17. Bell, J.T.; Biggers, R.E. *J. Molec. Spec.* **1968**, 25, 312.
18. Coyne, L.M.; McKeever, S.W.S. in <u>Spectroscopic Characterization of Minerals and Their Surfaces</u>, L.M. Coyne, S.W.S. McKeever, and D. F. Blake (eds.), ACS Press, Washington, DC (1990), Chapter 1.
19. Hochella, Jr., M.F.; White, A.F. (eds.) <u>Mineral-Water Interface Geochemistry</u>, Mineralogical Society of America, Washington, DC (1990).
20. Van Olphen, H.; Fripiat, J.J. (eds.) <u>Data Handbook for Clay Materials and Other Non-Metallic Minerals</u> Pergaman Press, New York (1980).

21. Bish, D.L. *U.S.DOE/OCRWM Yucca Mountain Project Report* **1989** TWS-ESS-DP-25.

22. Lytle, F.W.; Greegor, R.B.; Sandstrom, D.R.; Marques, D.R.; Wong, J. Spiro, C.L.; Huffman, G.P.; Huggins, F.E. *Nucl. Inst. Meth.* **1984**, *226*, 542.

23. Combes, J-M.; Chisholm-Brause, C.J.; Brown, Jr., G.E.; Parks, G.A.; Conradson, S.D.; Eller, P.G.; Triay, I.R.; Hobart, D.E.; Meijer, A. submitted to *Environ. Sci. Tech.*

24. Teo, B.K.; Joy, D.C. (eds.) EXAFS Spectroscopy: Techniques and Applications Plenum Press, New York (1981)

25. Tsunashima, A.; Brindley, G.W.; Bastovanov, M. *Clays and Clay Minerals* **1981**, *29*, 10.

26. Taylor, J.C.; Mueller, A. *Acta Cryst.* **1965**, *19*, 536.

27. Baes, C.F.; Mesmer, R.E. The Hydrolysis of Cations Wiley, New York (1976), pp. 177-182.

28. This energy difference does not by itself represent compelling evidence for the absence of a hydrolysis mechanism. However, the emission data for this sample (see text) are dramatically different from those of the hydrolytic species (Ref. 17) and do rule out the hydrolysis mechanism in this case.

29. Heller, E.J. *Acc. Chem. Res.* **1981**, *14*, 368.

Table I. Extended X-ray Absorption Fine Structure Data for UO_2^{2+} and UO_2^{2+}/TBP Complexes in Solution and Sorbed onto SAz-1

	System	Equatorial Oxygens		Axial Oxygens	
		Coord. #	Bond Dist. (Å)	Coord.#	Bond Dist. (Å)
1.	$UO_2(NO_3)_2(S)$[a]	6.0	2.48	2.0	1.76
2.	$UO_2(NO_3)_2(S)$	6.2	2.48	1.8	1.75
3.	UO_2^{2+}(aq)[b]	9.1	2.40	1.9	1.75
4.	$UO_2(NO_3)_2$/TBP[c] in dodecane	5.8	2.47	2.0	1.75
5.	UO_2^{2+}(aq) on SAz-1	4.8	2.43	2.1	1.74
6.	$UO_2(NO_3)_2$/TBP on SAz-1	~6	2.38	2.4	1.75

[a] Neutron diffraction data from Ref. 26.
[b] ~0.5 M $UO_2(NO_3)_2 \cdot 6H_2O$ in H_2O
[c] ~0.1 M $UO_2(NO_3)_2 \cdot 6H_2O$ in 20% TBP/dodecane

11

Table II. Luminescence and Raman Spectral Parameters for UO_2^{2+} and UO_2^{2+}/TBP Complexes in Solution and Sorbed onto SAz-1

Luminescence

Sample	E_{00} (cm^{-1})	$\nu_{U=O}$ (cm^{-1})	ν_{other} (cm^{-1})
$UO_2^{2+}{}_{(aq)}$[a]	20460	870	350
$UO_2^{2+}{}_{(aq)}$ in SAz-1	19950	840	-
UO_2^{2+}/TBP in SAz-1	20080	750	-

Raman

Sample	$\nu_{U=O}$ (cm^{-1})	ν_{other} (cm^{-1})
$UO_2^{2+}{}_{(aq)}$[a]	873	1050
$UO_2^{2+}{}_{(aq)}$ in SAz-1	855, 881	708
UO_2^{2+}/TBP in $C_{12}H_{26}$[b]	861	1031

[a] ~0.5 M $UO_2(NO_3)_2 \cdot 6H_2O$ in H_2O

[b] ~0.1 M $UO_2(NO_3)_2 \cdot 6H_2O$ in 20% TBP/dodecane

Figure Captions
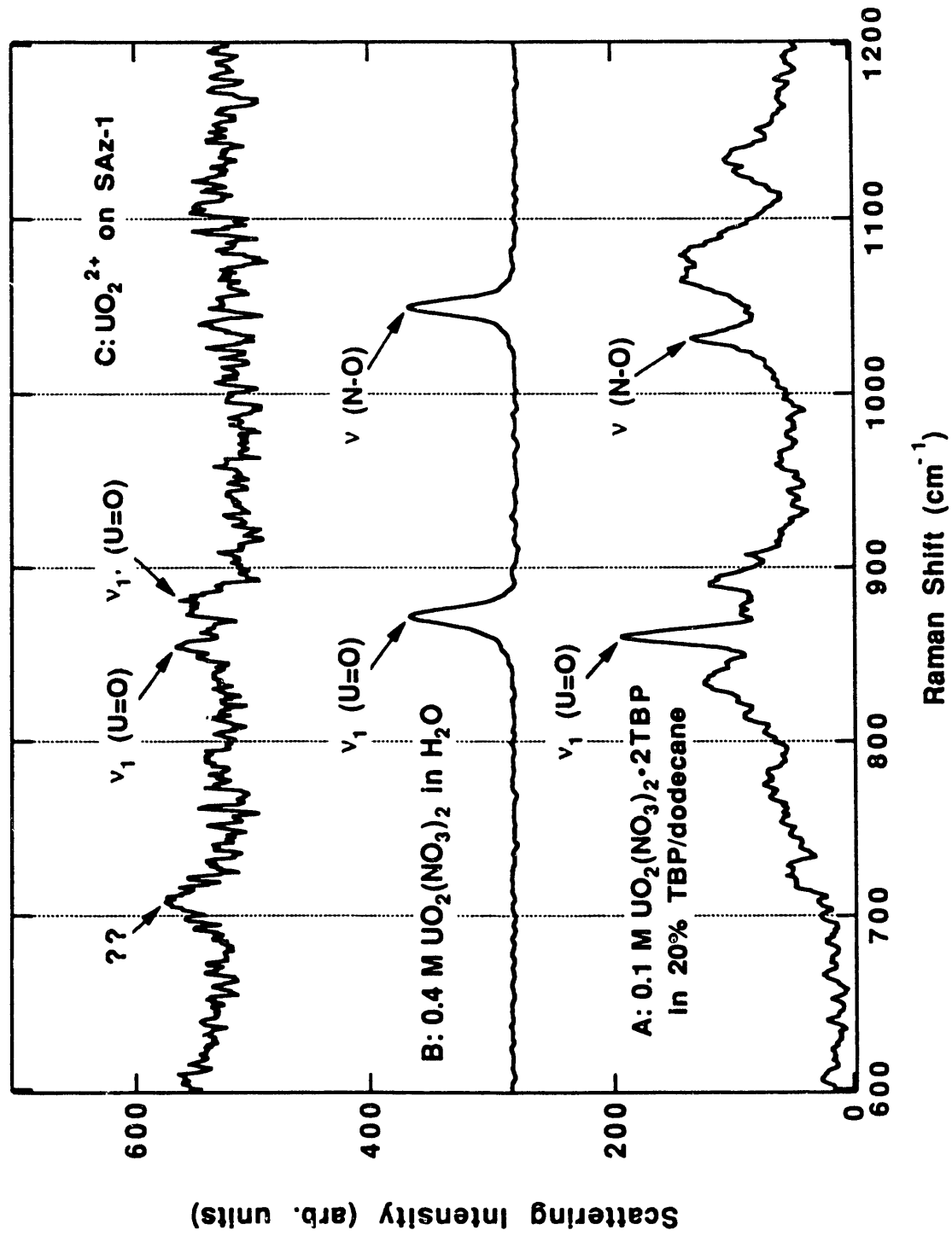
Figure 1.   Extended x-ray absorption fine structure radial structure functions for UO_2^{2+} species. (A) Solid $UO_2(NO_3)_2 \cdot 6H_2O$. (B) 0.5 M $UO_2(NO_3)_2 \cdot 6H_2O$ in aqueous solution. (C) 0.1 M $UO_2(NO_3)_2 \cdot 6H_2O$ in 20% TBP/dodecane. (D) UO_2^{2+} intercalated into SAz-1 from 0.5 M $UO_2(NO_3)_2 \cdot 6H_2O$ in aqueous solution. Each plot shows two separate data sets to demonstrate the reproducibility.

Figure 2.   Raman spectra of (A) ~0.1 M $UO_2(NO_3)_2 \cdot 6H_2O$ in 20% TBP/dodecane, (B) 0.4 M $UO_2(NO_3)_2 \cdot 6H_2O$ in aqueous solution, and (C) an air-dried powder sample of SAz-1 treated intercalated with aqueous UO_2^{2+} (as the nitrate salt). The unlabelled bands in (A) are from TBP and/or dodecane. The mode at ~ 708 cm^{-1} in (C) is unassigned.

Figure 3. Luminescence spectra of UO_2^{2+} species. (A) 0.4 M $UO_2(NO_3)_2 \cdot 6H_2O$ in aqueous solution. (B) Air-dried powder sample of SAz-1 intercalated with aqueous UO_2^{2+} (as the nitrate salt). (C) ~0.1 M $UO_2(NO_3)_2 \cdot 6H_2O$ in 20% TBP/dodecane. (D) Air-dried powder sample of the TBP complex of UO_2^{2+} intercalated into SAz-1. Note that the ordinate scaling factor for spectrum (C) is 1/10 that of the other spectra. All spectra were obtained using 363.8 nm CW Ar+ laser excitation and are not corrected for spectrometer or detector response. The structure seen on the high energy side of the emission band in (C) is Raman scattering from the solution.
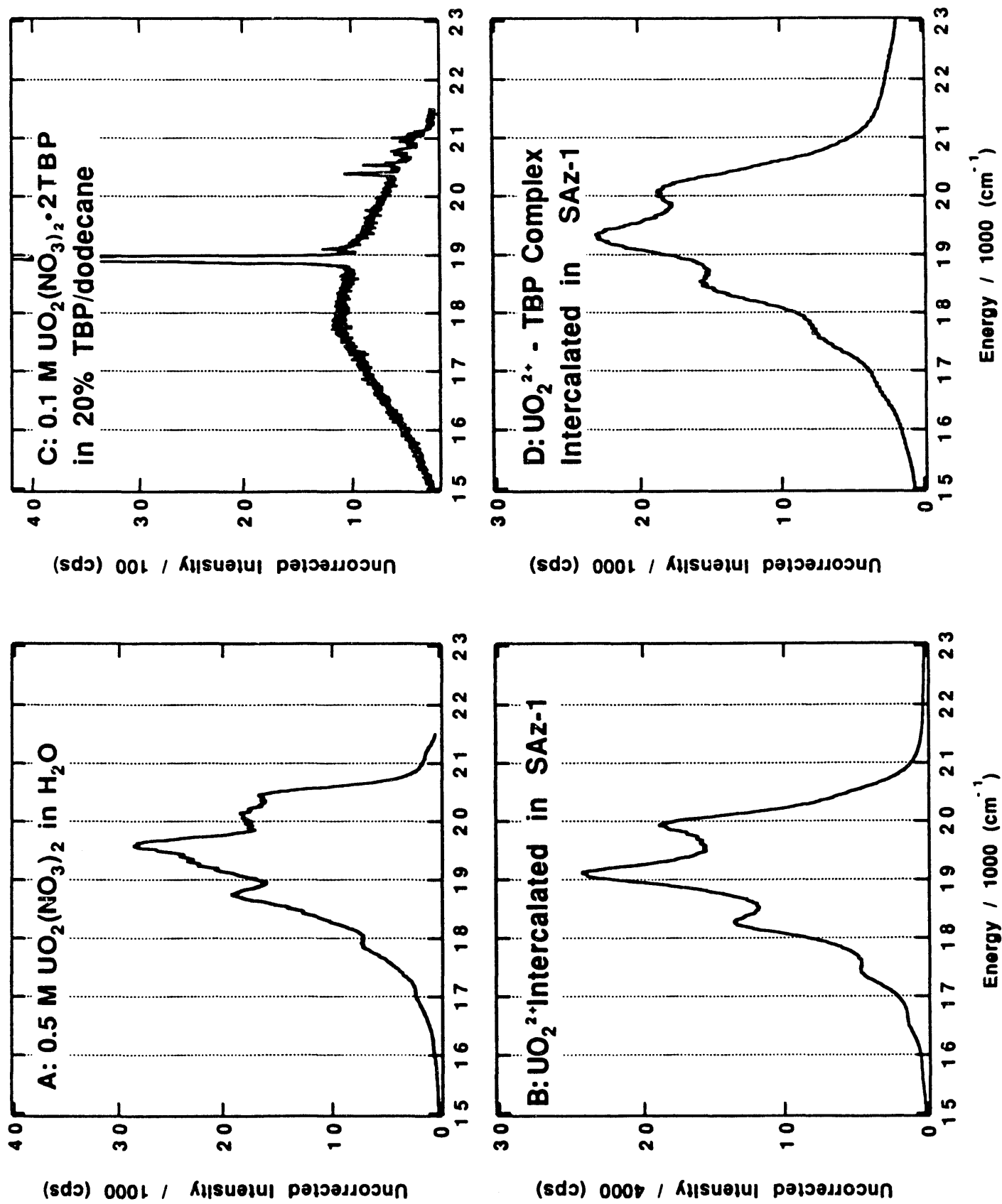
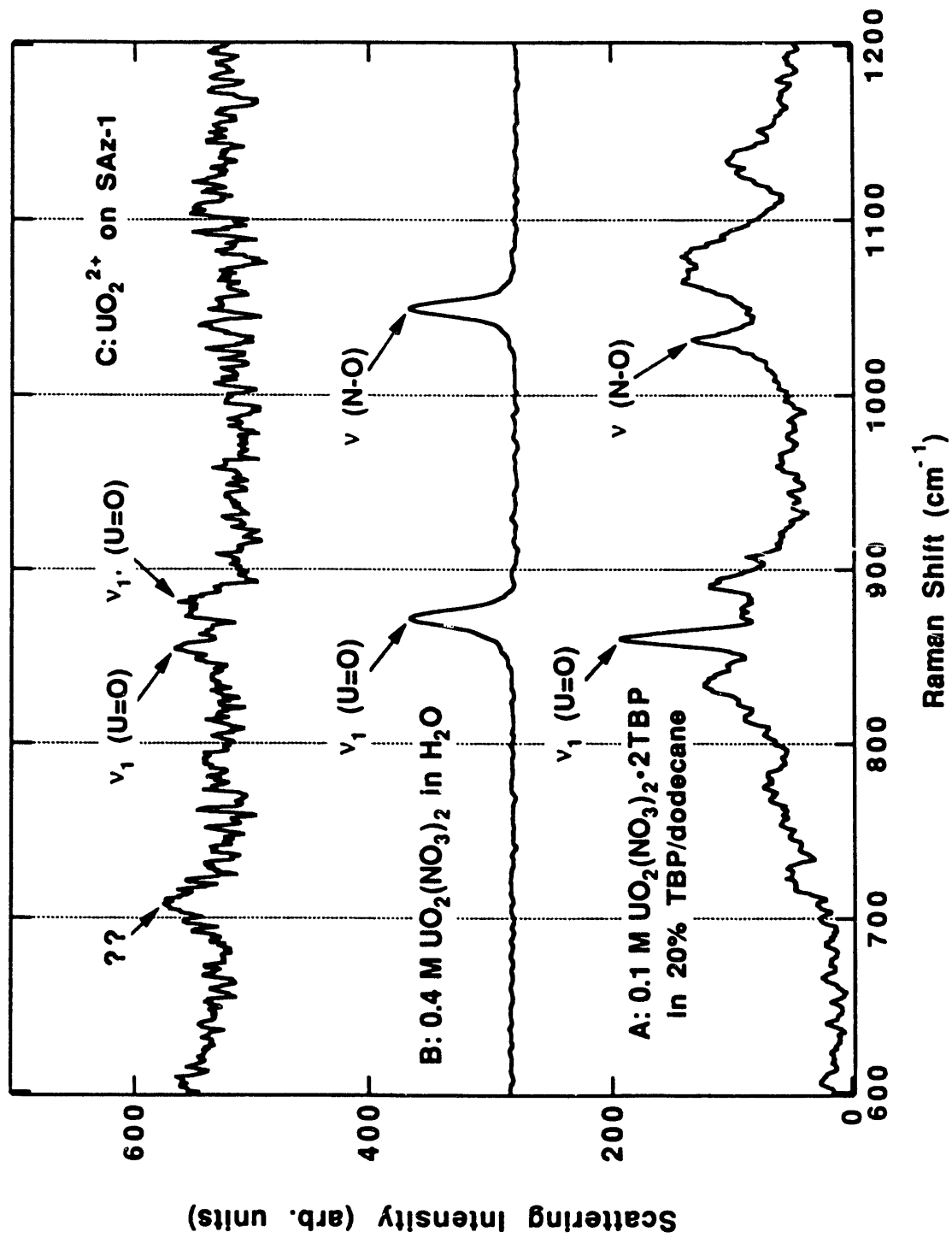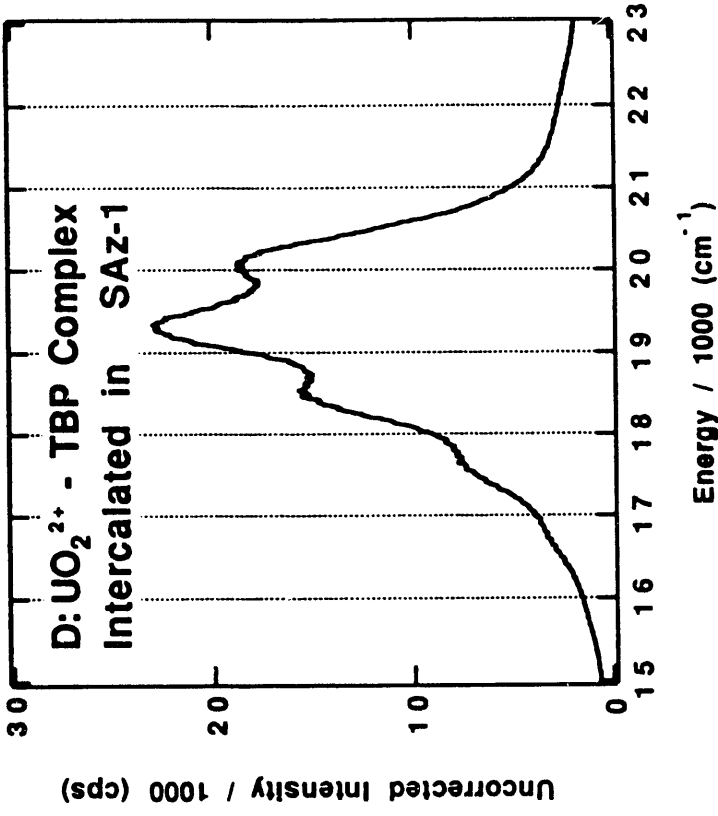**A:** $UO_2(NO_3)_2 \cdot 6H_2O$ (solid)

B: 0.5 M $UO_2(NO_3)_2$ In H_2O

C: 0.1 M $UO_2(NO_3)_2 \cdot 6H_2O$ In 20% TBP/dodecane

D: UO_2^{2+} Intercalated In SAz-1

Fourier Transform Magnitude

r (Å)
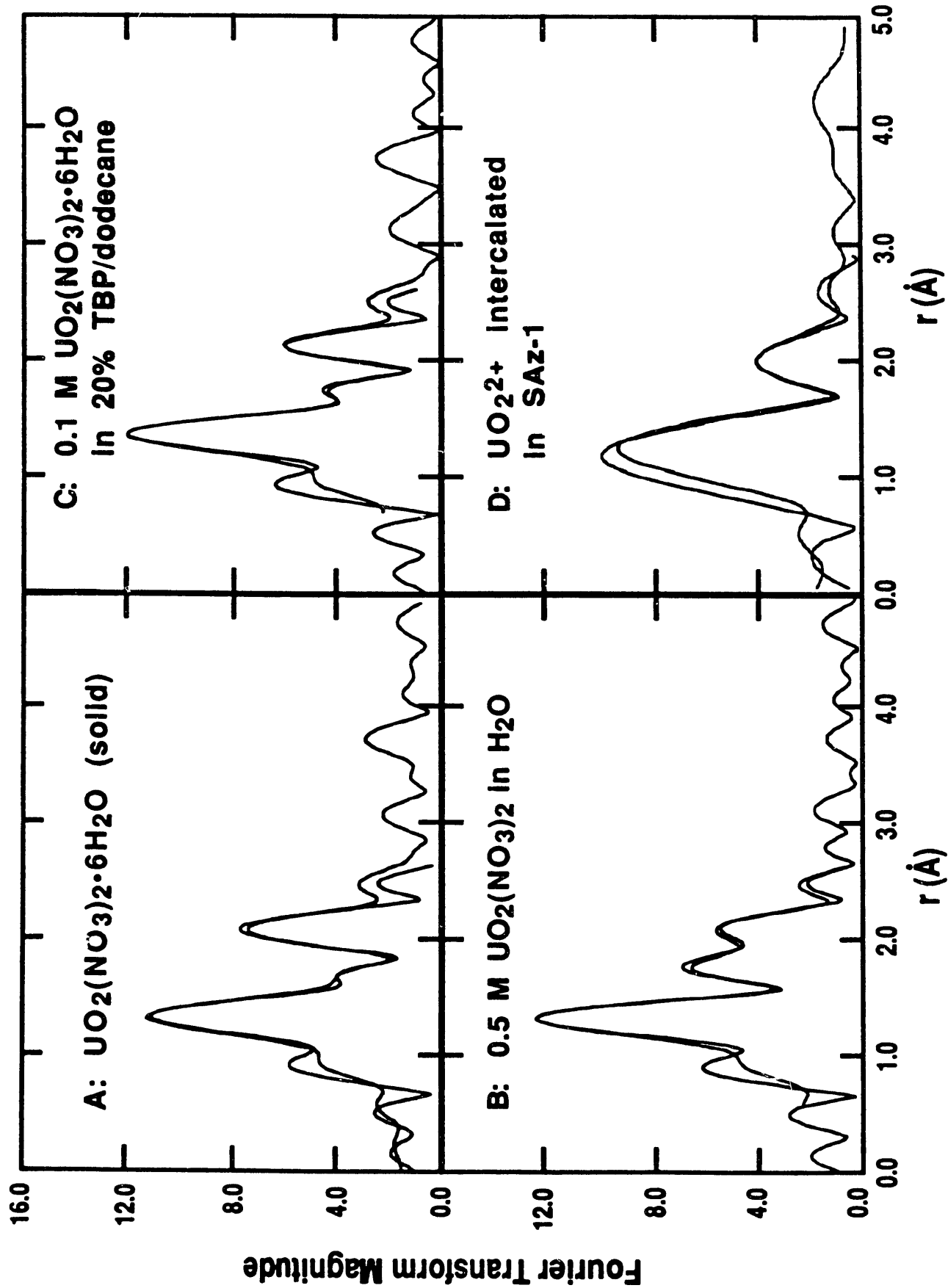
FIGURE 1

FIGURE 2

FIGURE 3

FIGURE 2

FIGURE 3

A: 0.5 M UO₂(NO₃)₂ in H₂O

B: UO₂²⁺Intercalated in SAz-1

C: 0.1 M UO₂(NO₃)₂·2TBP in 20% TBP/dodecane

D: UO₂²⁺ - TBP Complex Intercalated in SAz-1

END

DATE
FILMED

12/17/91